ISSN 0946-6010

BUNDESAMT FÜR
SEESCHIFFFAHRT
UND
HYDROGRAPHIE

Improvement of water level forecasts for tidal harbours by means of model output statistics (MOS)

Part I
(Skew surge forecast)

Berichte des BSH 47

BUNDESAMT FÜR
SEESCHIFFFAHRT
UND
HYDROGRAPHIE

Improvement of water level forecasts for tidal harbours by means of model output statistics (MOS)

Part I
(Skew surge forecast)

Autoren:

Sylvin H. Müller-Navarra

Bundesamt für Seeschifffahrt und Hydrographie (BSH), Bernhard-Nocht-Straße 78,
D-20359 Hamburg, E-Mail: mueller-navarra@bsh.de

Klaus Knüpffer

Meteo Service weather research GmbH (MSWR), Teltower Damm 25,
D-14169 Berlin

Berichte des
Bundesamtes für Seeschifffahrt und Hydrographie
Nr. 47/2010

In der Reihe „Berichte des Bundesamtes für Seeschifffahrt und Hydrographie“
werden Themen mit Dokumentationscharakter aus allen Bereichen des BSH veröffentlicht.
Durch die Publikation nimmt das BSH zu den Inhalten der Beiträge keine Stellung.
Die Veröffentlichungen in dieser Berichtsreihe erscheinen nach Bedarf.

Improvement of water level forecasts for tidal harbours by means of model output statistics (MOS)
im Internet: **www.bsh.de** (Menü: Produkte → Bücher → Berichte des BSH)

Hamburg und Rostock 2010
www.bsh.de

ISSN-Nr. 0946-6010

Contents

Abstract

The model output statistics (MOS) method has been used successfully in meteorological forecasting since the 1970s. Up to now, this method has never been used to predict water levels on marine coasts. Model systems combining numerical atmospheric and water level models have been in operational use since the 1980s and provide reliable water level forecasts. In operational applications, model predictions are modified manually (man-machine mix) before making them available to users. Growing demands on the quality of forecasts for shipping, especially forecasts for open tidal harbours, now require a definite improvement in the accuracy of predictions for periods ranging from 1 to 24 hours. On the example of the German tidal harbour of Cuxhaven, located on the mouth of the river Elbe downstream of Hamburg, it is demonstrated how the quality of predictions can be improved by applying the MOS method. This also opens up new possibilities for automated water level forecasting.

Zusammenfassung

Die Methode Modellausgabe-Statistik (MOS) hat sich in der meteorologischen Vorhersagepraxis seit den 1970er Jahren bewährt. Für Zwecke der Vorhersage des Wasserstandes an Meeresküsten ist dieses Verfahren bisher noch nicht angewandt worden. Modellsysteme aus numerischen Atmosphären- und Wasserstandsmodellen werden seit den 1980er Jahren operationell betrieben und liefern brauchbare Wasserstandsvorhersagen. In der Praxis werden die Modellvorhersagen manuell modifiziert (Man-Machine-Mix), bevor sie an Benutzer weitergegeben werden. Gestiegene Anforderungen an die Vorhersagen für die Seeschifffahrt, besonders für offene Gezeitenhäfen, erforderten nun eine deutliche Verbesserung der Vorhersagegenauigkeit im Vorhersagezeitraum 1 bis 24 h. Am Beispiel des deutschen Tidehafens Cuxhaven, in der Elbmündung stromab von Hamburg gelegen, wird gezeigt, wie durch Anwendung der MOS-Methode bessere Vorhersagen ermöglicht werden. Damit ergeben sich nun auch neue Möglichkeiten der Automatisierung von Wasserstandsvorhersagen.

Key words: water level forecasts, model output statistics, tidal river, North Sea

Acronyms:

BSH	Bundesamt für Seeschifffahrt und Hydrographie *(Federal Maritime and Hydrographic Agency)*
COSMO-EU	Europe model of DWD, gridpoint spacing 7 km, prediction period 3 days
DMO	Direct model output (skew surge of the 2Dv4 model)
DWD	Deutscher Wetterdienst
GFS	Global Forecast System
GME	Global model of DWD, gridpoint spacing 40 km, prediction period 7 days
HW, NW	High water, low water
MMM	Man-machine mix
MOS	Model Output Statistics
MSE	Mean Square Error
MSWR	Meteo Service Weather Research GmbH
RMSE	Root Mean Square Error
RV	Reduction of error variance
T	Current point in time
2Dv4	Two-dimensional wind surge model, version 4

1 Introduction

In many marine harbours around the world, shipping restrictions apply due to shallow water depths. Exact knowledge and reliable predictions of meteorological and oceanographic conditions are indispensable to ensure safe navigation in pilotage waters. The physical factor most relevant in this regard is the water level, which fluctuates periodically about a mean value due to tidal influence, and aperiodically mainly due to meteorological factors. The water depth available to a vessel is computed by addition of the current local water level referred to local chart datum and the water depth shown in the navigational chart, allowing for some under-keel clearance. Water level predictions for deep draught vessels must be very accurate in order to be able to define precisely the tidal window that is required, for example, to navigate a shoal area. Water level predictions for Cuxhaven are of extreme importance for the harbour of Hamburg, located 100 km upstream, and for navigation between these harbours. The tidal range at the Cuxhaven gauge station is 3 m; the time of tidal high water is 11 hours and 49 minutes after the moon's transit at Greenwich. Meteorological factors may cause water levels to rise by more than 3.5 m or to fall by more than 2.5 m. The influence of freshwater discharge from the upper reaches of the Elbe is just a few centimetres, even in case of extremely large discharge volumes (RUDOLPH, 2005). Storm surges causing water levels to rise more than 1.5 m above mean high water (MHW) occur in less than 0.6% of all cases (period from 1959 to 2008).

Deviations of tidal high or low water levels from the astronomically computed levels are called wind surge or wind set-up. The measured times of occurrence of high water and low water never correspond exactly to the astronomically predicted times. In this context, surge is defined as the difference between the astronomically computed high and low water levels and the relative extreme values of the measured water level curve. This value is also called “skew surge” (GERRITSEN et al., 1995). The numerical method uses an analogous approach; here, too, one model variation uses both tidal and meteorological forcing to simulate measured water levels, the other one is identical but excludes meteorological forcing. The skew surge value is determined for each grid point of the model area and is used as DMO in the BSH-MOS process. Surge values at Cuxhaven depend primarily on wind conditions in the central German Bight.

Frequency distributions of wind speeds and wind directions measured in the area have shown that wind speeds from 4 to 10 m/s (8 – 20 kn) occur in more than 50% of all cases, and that the prevailing wind directions are SW – W. Simple wind surge graphs can be prepared (MÜLLER-NAVARRA and GIESE, 1999) using only wind speed and wind direction as input (Fig. 1).

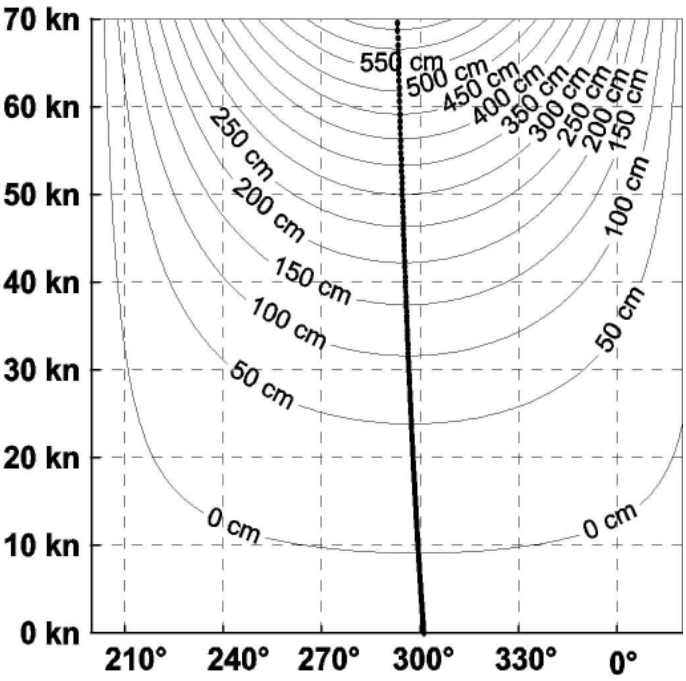

Fig. 1: Wind surge graph for Cuxhaven (onshore winds, after MÜLLER-NAVARRA and GIESE, 1999)

Strictly speaking, such surge graphs apply only under stationary conditions when circulation dynamics in the German Bight, after one or two days, have adapted to the wind field (KOLTERMANN and LANGE, 1975).

Tide tables for marine harbours based on astronomical predictions have been in use for a long time (ANON., 1878). Also the influence of weather on water levels had been recognised very early (ORTT, 1897). But it took a refined synoptic method to obtain fairly reliable wind forecasts for the open sea (SCHERHAG, 1948), which later, since the middle of the 20th century when high-performance remote data transmission became available, have led to relatively good water level forecasts for the German coastal waters and marine harbours (MÜLLER-NAVARRA, 2009a). Today, water levels in the German Bight are predicted using both empirical methods and numerical models (MÜLLER-NAVARRA et al., 2003), which are linked by a human interface (man-machine mix, MMM).

Analysing the prediction error, expressed as root mean square error (RMSE), for different prediction periods in the time from 2003 to mid-2009, it has been found that the quality of model predictions for a period of up to 15 hours can be improved by applying a man-machine mix (MMM). Beyond that, it has not been possible to further improve the direct model output (DMO) of the 2-dimensional model (DMO-2D) by human intervention (Fig. 2). The 2D model has been optimised for water level prediction applications; the RMSE of the 3-dimensional model (DMO-3D) generally is more than 2 cm greater in most cases. Besides, because of its longer computation time, the 3D model does not use weather predictions prior to the twelfth prediction hour.

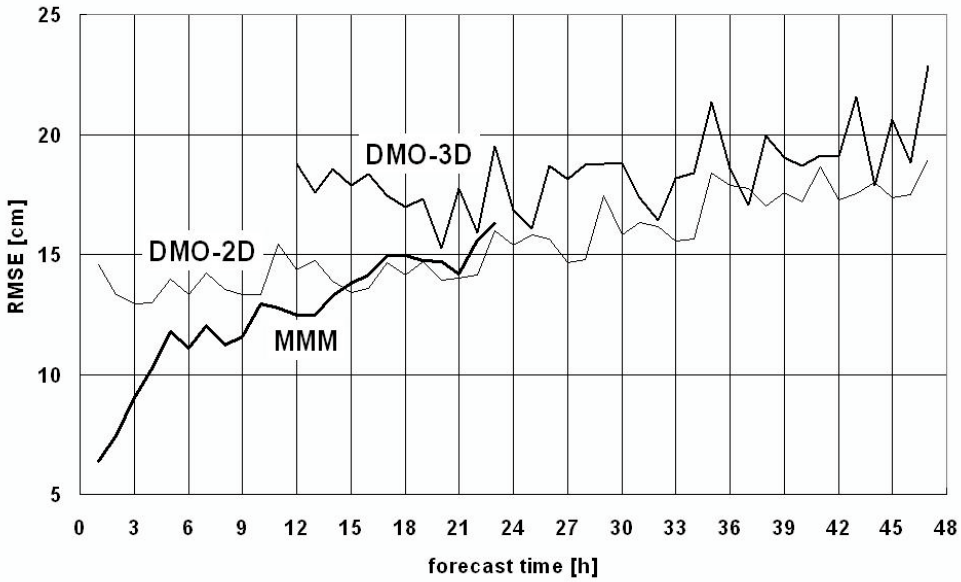

Fig. 2: RMSE (cm) of DMO (-2D and -3D, version 3: 1/2003 – 12/2007, version 4: 1/2008 – 8/2009) and MMM. Cuxhaven harbour. Number of cases for each forecast time: MMM: about 1500, DMO-2D: 700, DMO-3D: 350.

It will be demonstrated in this paper, on the example of the river Elbe with its heavy traffic of seagoing ships, that a marked improvement of water level predictions for the harbour of Cuxhaven can be achieved by applying model output statistics (MOS), i.e. by subsequently applying statistics-based corrections. The model output statistics (MOS) method has been used successfully in meteorological operational forecasting since the 1970s (GLAHN et al., 1972). This novel method of predicting wind surge will be called BSH-MOS in the following.

2 Available direct model output from the DWD-BSH model chain

In situations of rapidly changing wind conditions, numerical model systems combining atmospheric and circulation models have been found to provide better results than empirical methods. Such model systems covering the German Bight have been in operational use at Bundesamt für Seeschifffahrt und Hydrographie (BSH) since 1981 (SOETJE and BROCKMANN, 1983). In 1990, the model was extended to cover the entire area of the North Sea and Baltic Sea. Today, 3D hydrodynamic-numerical ocean and shelf sea models predict numerous physical variables (Dick et al., 2001), among them water levels. If only water levels are of interest, a 2D model is sufficient. It requires considerably less computation time than the 3D model. The lower computation time is an important advantage for MOS because it allows timely inclusion of all forcing data provided by atmospheric models. The BSH receives hourly predictions of meteorological parameters from the GME/COSMO-EU modelling chain of DWD four times a day (MAJEWSKI et al., 2002; STEPPELER et al., 2003).

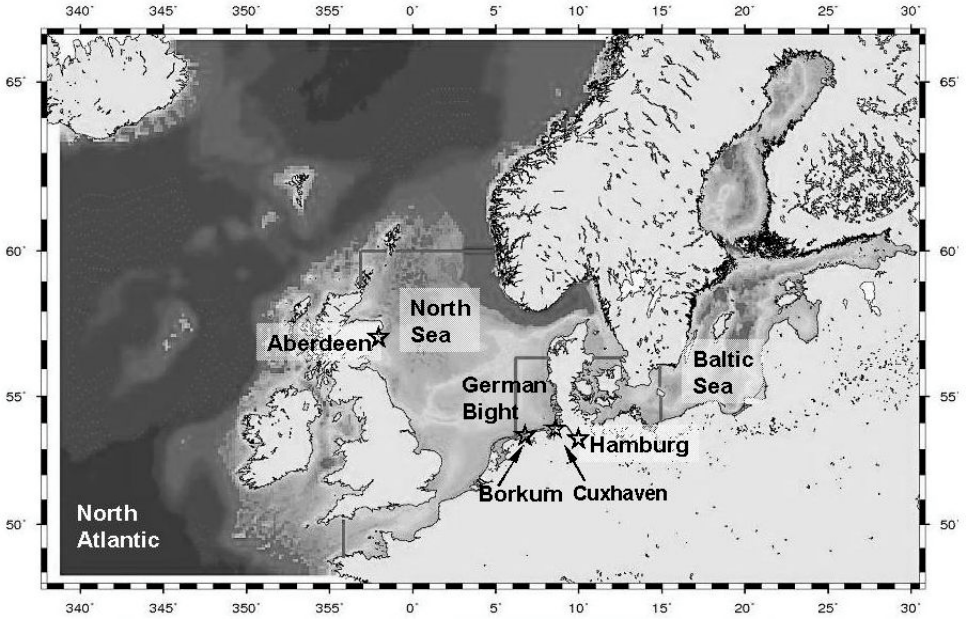

Fig. 3: Model areas of BSH's numerical water level forecast system

The analysis for the MOS equations was made on the basis of a data set covering the period from January 2008 to July 2009, using the 0 and 12 h runs of the 2D model (DMO: 2Dv4). The model system currently used in BSH-MOS, version 4, presently has the following configuration:

– Meteorological input data from GME/COSMO-EU

– Double nested [3D: triple]
  - Northeast Atlantic model (20 km grid size)
  - North Sea model (5.5 km), [3D: North and Baltic Seas model]
  [- 3D: coastal model, German Bight and Western Baltic (0.9 km)]

– 4 runs per day (starting at 0, 6, 12, and 18 UTC), [3D: 1 daily run (12 UTC)]

The 3D model configuration is given alternatively or additionally in square brackets.

In the forecasting modus, new surge prediction data from DMO-2D in the v4 version (2Dv4) enter the MOS equations every six hours.

3 Model output statistics MOS

With regard to standard weather elements, MOS reduces about 50% of the error variance of Direct Model Output predictions for particular predictands (weather elements) (KNÜPFFER, 1999). Subsequent verification has shown that this ratio has been unchanged in the past 10 years: numerical models have improved, MOS methods have improved as well, and the relative difference between the RMSE values of DMO and MOS has remained more or less unchanged. Other successful MOS applications are nowcast applications such as lightning, radar, and cellMOS, and their integration into the automated WarnMOS forecasting systems of DWD (HOFFMANN, 2008) and in aviation weather forecasting systems (e. g. Auto-TAF, {KNÜPFFER, 1997}), predictions of wind speeds, pollutant concentrations (particulate matter, ground-level ozone) water levels of rivers, among many others. Generally speaking, MOS applications always are promising in predictions of parameters depending essentially on the weather, and for which long-term observation series are available. The success of MOS is generally attributable to intelligent coupling between the predictions of numerical weather prediction models and observation data. In MSWR-MOS, this has been achieved particularly by linearising the frequently non-linear relationships between predictors and predictand via analytical and empirical transformations. An interesting question concerning surge predictions was whether, in view of the existence of a high-performance 2D model (as DMO) whose prediction quality only in the first 15 forecasting hours has been surpassed by the oceanographers of the forecasting service, it would be possible to achieve comparable quality improvements using MOS. After completion of the development phase and 6½-month operational use, this question can be answered as follows: the development results suggest the possibility of a 60% reduction of the error variance RV(MOS,DMO) which is defined as follows:

$$RV(MOS, DMO) = 100\% \cdot (MSE_{DMO} - MSE_{MOS}) / MSE_{DMO} \quad (1)$$

Operationally about 40% RV has been achieved so far. Even in the hypothetical case that further improvement is not feasible, the project may be considered a full success because 10% RV generally is considered a noticeable improvement. The following rule of thumb illustrates the effect of RV: 1% RV corresponds to one hour additional predictability at unchanged prediction quality. A method improving another method's forecast by 24% RV thus generates predictions for T+dt+24 hours whose RMSE is comparable to that of the T+dt hours predicted before.

3.1 Most important groups of predictors

MOS equations are developed for hourly output and for prediction periods of up to T+33 hours, i.e. typically for the next 5 to 6 times of tidal high and low water. In the North Sea, which is dominated by semidiurnal tides, the average time between two tidal high waters is 12.42 hours. Duration of rise and fall normally is not equal: tidal rivers have a reduced duration of rise, with duration of fall reduced accordingly. Depending on the number of hours between the time of MOS prediction output and the times of high or low water, suitable coefficients for the 5 to 6 matching times are taken from 33 available equations. The predictor „wind surge" at the required gauge stations is determined automatically at the times of high and low water, i. e. it is not available continuously (MÜLLER-NAVARRA, 2009b).The most important groups of predictors (in about the sequence of their linear correlation to the predictand) are:

1. Latest surge observation at Borkum, best correlated (about 0.97) only for T+1 and T+2 because a particular surge event occurs 2 - 3 hours earlier at Borkum than at Cuxhaven.

2. DMO surge forecast (2Dv4), with meteorological input from GME/COSMO-EU of DWD. Correlation decreasing from 0.94 to 0.88 between T+1 and T+33 h.

3. Persistence of last observation: (auto-) correlation of the predictand decreasing rapidly from 0.81 to 0.3 between T+1 and T+33 h.

4. Wind surge: wind components of 295 ±10 degrees and exponent 1, 1.5 or 2 derived from GFS model (KALNAY et al., 1990). Correlations from 0.8 to 0.7.

5. Basic set of other GFS predictors and derived variables (about 150 potential predictors) with best correlations from 0.75 to 0.65 for U components of (geostrophic) wind between 950 hPa and 10 m above mean sea level.

6. Wind surge observations at Aberdeen in its double function as a signal provider for external surges coming in from the Atlantic Ocean (CORKAN, 1950) and provider of general information about the North Sea's current water volume, with correlations from 0.6 to 0.5. External surges are measurable at the Cuxhaven gauge after about 12 hours.

7. *Pers2D_korr:* this is the most important predictor in the system: the correction of the last known initialisation error of the 2D model. Correlation of predictor and predictand is low, but correlation of the predictor with the residuum (error) of the 1-predictor MOS equations with the initialisation error of DMO of the last corresponding surge event in some cases is greater than 0.6.

In the discussion of MOS equations below, the symbiosis of physics (2Dv4 model and GFS model), synoptics (in the selection and transformation of predictors), and statistics (multiple linear screening regression) has been described exemplarily. The standard MSWR regression table format used for this purpose has only been explained to the extent required to understand the explanatory texts. A more detailed description of the table outputs is provided in KNÜPFFER (1996) and HOFFMANN (2008).

3.2 Predictands

The following predictands are forecast:

Surge	unclassified predictand	
SurgeH	high water surge	classified by HW/LW
SurgeL	low water surge	classified by HW/LW
Surge+	positive surge	classified by surge+/surge-
Surge-	negative surge	classified by surge+/surge-
StH+	surge+ at HW	classified by StH+/StH-/StN+/StN-
StH-	surge- at HW	classified by StH+/StH-/StN+/StN-
StL+	surge+ at LW	classified by StH+/StH-/StN+/StN-
StL-	surge- at LW	classified by StH+/StH-/StN+/StN-
Kombi	Suitable combination of the latter four predictands if ABS(surge - 4 cm) > 2**Abs_Err_surge*, otherwise Kombi=surge. Abs_*Err_surge* is the MOS-computed absolute error of the MOS prediction of the surge predictand.	

Table 1: Predictors referred to in the text. The total number of potential predictors used in the analyses is about 250.

Acronym	Description	Source
BrkLastStau	Last surge observed at Borkum island gauge	Tide gauge
BrkLastStau-1 (-2, -3, ...)	Next to the last (third, fourth ... to the last) surge observed at the Borkum island gauge	Tide gauge
Last2DModel	Last available DMO wind surge prediction for the Cuxhaven gauge	2D model
Pers2D_korr-2	Next to the last (third, fourth ... to the last) known initialisation error of the 2D model	2D model and tide gauge
*WSt1_295**2*	Squared 295-degree-component of geostrophic 1000-hPa wind	GFS model
Fl_1000	Geopotential 1000 hPa	GFS model
AbrLastStau	Last wind surge observation Aberdeen	Tide gauge
DMO_DD_SE	SE component of DMO 10m wind	GFS model
Fl_0Cisotherm	Geopotential of the 0 degree isothermal line	GFS model
4Lev_Lift_Ix	4-Level-Lifted index	GFS model
*WStLS_295**2*	Squared 295-degree component of DMO 10m large-scale wind	GFS model
Rot_1000/FF1000	Eddy size in 1000 hPa divided by wind speed in 1000 hPa	GFS model
U_300	U-component of geostrophic wind in 300 hPa	GFS model
*Cos_2*Dag*	Cosine of the day in half-year	Date

4 Development results

There are two basically different forecast phases.

Tab. 2: Regression table of Phase 1, T+1 h.

Predictand Surge, output time T 05 UTC, prediction time T + 1 h:

MV	SD	R_Pd	R_Res	Name	dRVI	Co	Wgt	Ctr
5.9	30.9	0.970	0.970	*BrkLastStau*	94.1	0.77	51	63
208.8	587.3	0.769	0.480	*WSt1_295**2*	41.8	0.01	9	9
10.2	34.2	0.943	0.072	*Last2DModel*	5.1	0.34	25	30
-3.3	12.1	0.213	0.322	*Pers2D_korr-2*	14.0	0.17	4	1
5.9	30.8	0.765	-0.140	*BrkLastStau-1*	5.1	-0.07	-5	-5
111.6	89.6	-0.328	0.194	*FI_1000*	4.3	0.02	3	-1
-3.3	12.0	0.185	0.142	*Pers2D_korr-4*	3.0	0.12	3	1

Const. =	-2.9	#Case rm=	1639	340	RV(HC) =	98	SD%(8) = 7
MV(Pd) =	6.9	#pC eC =	1609	1639	E(RVI) =	98	RMSE = 5.6
SD(Pd) =	36.5	#pPr/Rj =	254	17	krit_R =	0.078	E(RMSI)= 5.74

The last HW or LW surge at Borkum – determined not later than one hour before output time – is an excellent indicator of the surge level to be expected at Cuxhaven. Being the best-correlated predictor, it is selected first by the regression algorithm. The dRVI column contains the values of the expected reduction of the error variance due to integration of the particular predictor into the equation.

In the case of the first predictor, this value is 94.1% of the initial variance of the predictand of SD(Pd)2=(36.5 cm)2. The error of the 1-predictor equation with BrkLastStau is corrected most effectively, with the error variance reduced by more than 40%, by wind surge computed on the basis of the square of GFS-predicted geostrophic 1000 hPa wind from a 295° direction (WNW). The next predictor is the last 2D model and the correction of its last known initialisation error, which has been discussed in more detail in the explanations to phase 2 below. The next-to-last surge in Borkum (BrkLastStau-1) is used with a negative sign; together with BrkLastStau, it forms a trend equation. A further 4.3% reduction of the remaining error variance is achieved by the geopotential in 1000 hPa, and another 3% by correcting the model's initialisation error for the next-to-last corresponding surge event. It is apparent from the Wgt column, which shows the predictor weighting standardised to 100% (with the sign of the regression coefficient Co), that BrkLastStau accounts for well over 50% of the total reduction of the error variance of this equation, followed by DMO, at 25%, and GFS wind surge at just under 10%. The other predictors account for the remaining 15% of weighting. The MOS equations for T+2 hours are of comparable quality. The weight percentages add up to 100%, the values in the Ctr column (contribution) to RV=98%, and dRVI according to the above formula:

$$RVI = (1 - \prod [1 - dRVI_i / 100\%]) \cdot 100\% \quad (2)$$

In equation (2) $dRVI_i$ designates the reduction of the error variance due to integration of the new i^{th} predictor.

Tab. 3: Regression table of Phase 2, T + 3 h.

Predictand Surge, output time T 05 UTC, prediction time T + 3 h

MV	SD	R_Pd	R_Res	Name	dRVI	Co	Wgt	Ctr
10.4	34.4	0.942	0.942	*Last2DModel*	88.6	0.90	65	79
-3.3	12.1	0.213	0.630	*Pers2D_korr-2*	39.3	0.40	10	3
-3.3	12.0	0.188	0.244	*Pers2D_korr-4*	9.2	0.29	7	2
5.5	15.8	0.583	0.130	*AbrLastStau*	1.9	0.14	5	4
-1.0	8.3	-0.647	-0.097	*DMO_DD_SE*	1.5	-0.26	-5	4
6.6	4.5	-0.253	-0.113	*4Lev_Lift_Ix*	0.9	-0.21	-2	1
9.8	33.5	0.382	-0.082	Last2DModel-4	0.2	-0.04	-3	-1
5.9	30.9	0.767	0.066	*BrkLastStau-1*	0.6	0.05	3	3

Const. =	0.4	#Case rm=	1641	337	RV(HC) =	94	SD%(8) = 6
MV(Pd) =	6.9	#pC eC =	1611	1641	E(RVI) =	94	RMSE = 8.7
SD(Pd) =	36.6	#pPr/Rj =	253	16	krit_R =	0.078	E(RMSI)= 8.93

From phase 2 (T+3 hours), DMO is the dominant predictor. It is followed by the predictor *Pers2D_korr* at the time of the last corresponding surge (HW with HW and NW with NW). This predictor includes the difference between the persistence of the predictand of the last (-1), next-to-last (-2) etc. surge event and the last available model prediction for this particular time. The model's initialisation errors at the time of the last corresponding surge are preferably used although they may be 6 hours further back than the most recent known initialisation error of the model. This points to its strong dependence on the tide (HW or LW). *Pers2D_korr* accounts for about half of the total reduction of the error variance of unclassified MOS as compared to DMO, i.e. for 24% of 46% averaged for all prediction periods. This indicates a surprisingly high persistence (temporal autocorrelation from output time to output time) of the model's initialisation error. Over selected prediction periods for the 4 observed surge events receding the selected output time of 05 UTC, the correlations of the *Pers2D_korr* predictors are distributed as follows:

Tab. 4: Correlation of the predictors Pers2D_korr-x to the residuum of the 1-predictor equation using the Last2DModel as predictor:

Fp	-1	-2	-3	-4
03	.16	.63	.15	.58
09	.59	.16	.55	.18
15	.16	.53	.18	.41
21	.50	.17	.39	.15
27	.17	.37	.14	.36
33	.36	.15	.36	.12

It is apparent from the dRVI column that by far the largest proportion of the performance of the MOS equation is attributable to consideration of this error: decreasing from 46% RV (according to the RV addition rules, 39.3% plus 9.2% RV is about 46%) in the equation for T+3 hours to 15% for T+33 hours. All other predictors are of lesser importance.

Tab. 5: Regression table of Phase 2, T + 33 h.

Predictand Surge, output time T 05 UTC, prediction time T + 33 h:

MV	SD	R_Pd	R_Res	Name	dRVI	Co	Wgt	Ctr
10.9	37.9	0.915	0.915	*Last2DModel*	83.6	0.78	64	74
-3.4	12.2	0.148	0.365	*Pers2D_korr-3*	12.8	0.24	6	1
16.9	10.4	-0.085	0.159	*FI_0Cisotherm*	2.2	0.19	4	0
25.2	102.9	0.750	0.097	*WStLS_295**2*	1.7	0.04	8	8
-4.1	23.8	0.145	0.140	*Rot_1000/FF1000*	1.5	0.09	5	1
-3.4	12.3	0.145	0.125	*Pers2D_korr-1*	2.0	0.21	6	1
27.3	31.9	0.524	0.089	*U_300*	0.5	0.06	4	3
-6.6	70.1	-0.057	-0.093	*Cos_2*Dag*	0.3	-0.02	-3	0

Const. =	-5.9	#Case rm=	1648	330	RV(HC) =	87	SD%(8) = 7
MV(Pd) =	6.6	#pC eC =	1621	1648	E(RVI) =	87	RMSE = 12.8
SD(Pd) =	36.3	#pPr/Rj =	259	16	krit_R =	0.078	E(RMSI)= 13.15

In the two equations, MOS reduces the error variance of DMO by about 50% (T+3h) and 35% (T+33h), see Table 7 below.

Classification of predictands

Experience gained in oceanographic operational applications has shown that HW and LW surges react differently to otherwise identical surge signals; accordingly, positive and negative surges are governed by different "rules" (prediction rules and experience). This led to the novel approach of making a classification based on the two criteria, initially 2x2 classes with HW and LW or surge+ and surge-, respectively, accounting for about half of all cases in a particular class; later and in operational use even 4 classes: HW+, HW-, LW+, LW-.

Averaged over all prediction periods analysed, an even higher reduction of variance has been achieved with classified predictands (28%) than by making allowance for the initialisation error of the 2Dv4 model with an unclassified predictand (26%). The improvement is mainly due to a more differentiated consideration of the role played by the inialisation error of DMO. For, consideration of the initialisation error is much more successful with negative surges than with positive surges, as can be seen in the Table 6 below:

Table 6: Reduction of the error variance of the Pers2D_korr predictors for the four classes, in %

LW+	HW+	LW-	HW-
8	19	39	52

MOS improvements to DMO thus are likely to be most successful with expected negative surges, particularly at high tide. Such results should be of interest to modellers looking for ways of improving their models. However, in order to preserve the quality of the DMO+MOS overall system, they should avoid changing their v4 models but, instead, use these diagnoses in developing a next v5 model version. Table 7 summarises the results obtained so far in verifying the development system – with regard to the importance of different groups of predictors – for selected prediction periods Fp:

Table 7: Contributions of different groups of predictors to the reduction of error variance, broken down into phase 1 (T+1 hour) and phase 2 (T+3, 9, ..., 27, 33 hours)

(1) Fp /h	(2) RMSE DMO	(3) RMSE MOS	(4) RV MOS	(5) RV MS1	(6) RV Bk	(7) RV GFS+S	(8) Prs2D _korr	(9) RV S p l i t HW/NW	(10) +/-	(11) Tot	(12) RV (MOS,DMO)
01	127	57	80	2	55	46	17	20	10	26	85
03	128	89	52	7	1	3	45	15	15	23	63
09	134	96	49	9	-	3	40	16	16	31	65
15	136	107	40	12	-	3	30	18	18	31	59
21	145	114	38	14	-	4	24	14	18	28	56
27	151	127	31	13	-	6	15	14	26	30	52
33	160	132	35	16	-	5	15	9	20	27	53
Ph2	142	111	39	12	0	4	27	14	17	28	56
Tot	140	103	46	11	8	10	26	15	16	28	61

The last two lines show the mean values of the RMSE and (RMSE weighted) RV values of phase 2 and corresponding mean values of both phases, respectively, i.e. all Fp considered. The individual columns include the following:

Column 2:	RMSE of DMO, mm.
Column 3:	RMSE of MOS without classification, mm.
Column 4:	Reduction of error variance of MOS without classification resulting from columns 2 and 3, compared to DMO; all RV data in percent.
Columns 5–8:	Percentage of the most important predictor groups in the total RV in column 4.
Column 5:	Reduction of error varance of 1-predictor equation using only DMO as predictor, compared to pure DMO.
Column 6:	Percentage of surge at Borkum.
Column 7:	Percentage of all 200 potential predictors from GFS and MSWR-MOS base technology, which additionally include astronomical, harmonic, and binary predictors.
Column 8:	Percentage of the correction of the last known initialisation error of DMO, already referred to above.
Column 9:	Further reduction of variance versus column 4 by splitting into HW/LW.
Column 10:	Further reduction of variance versus column 4 by splitting into surge+/surge-.
Column 11:	Total reduction of variance by splitting into the 4 classes HW+, HW-, LW+ and LW-. It is only approximately equal to the RV total of columns 9 and 10 because the 8 MOS equations involved are all computed independently from each other.
Column 12:	Total reduction of error variance RV (MOS, DMO) following classification as RV total of columns 4 and 11.

It is obvious that most of the reduction of DMO error variance (on average 50 of 61%) is due primarily to manipulation of DMO - not to additional external information such as observations or GFS prediction elements. In the long phase from T+3 to T+33 hours, this accounts for as much as 54 of 56% of the reduction of the error variance.

The main variance reducing components are:

1. Classification, at 28%.
2. Pers2D correction, with an average 26%, but decreasing strongly with increasing length of the prediction period, from 45% at T+3 hours to 15% at T+33 hours.
3. The 1-predictor MOS equation. It eliminates the systematic error of DMO, which is about +4 cm, and optimises the standard deviation of DMO through a coefficient not equal to 1. The coefficient in this equation decreases from 1.00 at Fp = 1 hour to 0.88 at Fp = 33 hours and, from about T+10 hours, it achieves 2-digit reductions in the percentage of variance with this incipient convergence towards the expected climatological value alone. Averaged over phase 2, this is as much as 12%.

DMO thus plays an outstanding role as a predictor. Unlike other MOS systems used, e.g., to forecast air temperatures, where the quality of MOS predictions mostly deteriorates only negligibly in the absence of DMO, and where DMO predictors rarely account for more than 50% of the total reduction of the error variance, the BSH MOS equations without DMO on average only would have the lower quality of pure DMO, with about 60% RV less.

Nevertheless, this is an excellent example of a symbiosis of physics and statistics.

5 Verification of 6½-months' operational forecasts

A comparison is made of DMO, combination forecasts (Kombi) and Surge, as well as Mix, an arithmetic mean of these three predictions. Wherever a man-machine mix of the BSH water level forecast service was available, it has been included in the verification. Four daily forecasts since the beginning of operational use, at 05, 11, 17 and 23 UTC in the format shown below (Tab. 8), were included in the evaluation. The forecasts made at other times hardly differ from those above because new DMO or GFS input is only available every 6 hours.

Tab. 8: Wind surge observations (fourth line) and forecasts (lines 5 – 9) for Cuxhaven harbour [cm] (left side) together with corresponding error squares [cm²] (right side). Forecasts are given with lead times 1 to 33 hours (second line) for three high and low waters (third line) after 20 August 2009, 23 UTC.

1	Cux: Issue: 20090820 23z				2D-Modell: 18z		GFS: 18z	Aberdeen: 18z				Borkum: 22z		
2	LeadT	1	8	13	20	26	33		1	8	13	20	26	33
3	HHMM	0025	0714	1236	1946	0112	0801		0025	0714	1236	1946	0112	0801
4	Obs	7	12	10	23	12	28							
5	MMM	1	7	15	15	7		175	36	25	25	64	25	
6	DMO	3	5	17	13	9	10	223	16	49	49	100	9	324
7	Mix	9	6	14	18	10	10	76	4	36	16	25	4	324
8	Kombi	13	7	9	23	10	10	66	36	25	1	0	4	324
9	Surge	12	7	16	17	10	10	126	25	25	36	36	4	324

The error squares of the predictions to the left are shown on the right side. The added values are in the middle, not taking into account the last column on the right side because no MMM was made for T+33h.

A complete evaluation of all prediction times from 14 July 2009 to 30 January 2010 results in the following RV reductions: DMO 0% (reference prediction); Mix 39%, Kombi 42%, Surge 39% (Tab. 9).

The verification period started with 1½ summer months of low dynamics and good results – though below expectations – followed by a long autumn season with mostly variable weather and westerly flow. DMO was extraordinarily accurate in this period, and MOS over-corrected its initialisation errors on average, which led to an RV(*,DMO) far below expectations. Only Mix was capable of reducing more than 10% error variance in autumn. The situation changed dramatically at the end of the verification period , when an unusually severe cold spell with prevailing E-SE winds set in. The model had huge initialisation errors which were easily corrected by MOS, resulting in a reduction of variance by more than ¾ during the last three weeks of the verification period.

Table 9: Sum of Squared Errors (SSE) and corresponding RV values in different time periods.

		RMSE/cm				RV(*,DMO)		
	n	DMO	Mix	Kombi	Surge	Mix	Kombi	Surge
14Jul09 - 01Sep09	981	10.2	8.5	8.0	8.9	30%	38%	23%
02Sep09 - 08Dez09	1960	11.5	10.7	11.2	11.2	14%	6%	6%
09Dez09 - 08Jan10	586	14.4	10.2	10.4	10.3	49%	48%	48%
09Jan10 - 30Jan10	429	24.5	14.6	11.8	12.0	64%	77%	76%
14Jul09 - 30Jan10	3956	13.7	10.6	10.4	10.6	39%	42%	39%

It turned out that Mix is the best choice in periods in which RV(Kombi, DMO) is lower than 25%. The surge predictand delivered operationally what the development phase had promised. Kombi would need another 30% RV to meet the expectations arisen from the development data. Follow-up investigations will show whether there is too much overfitting in the Kombi equations or whether the result will come closer to 60% with a prolonged verification period.

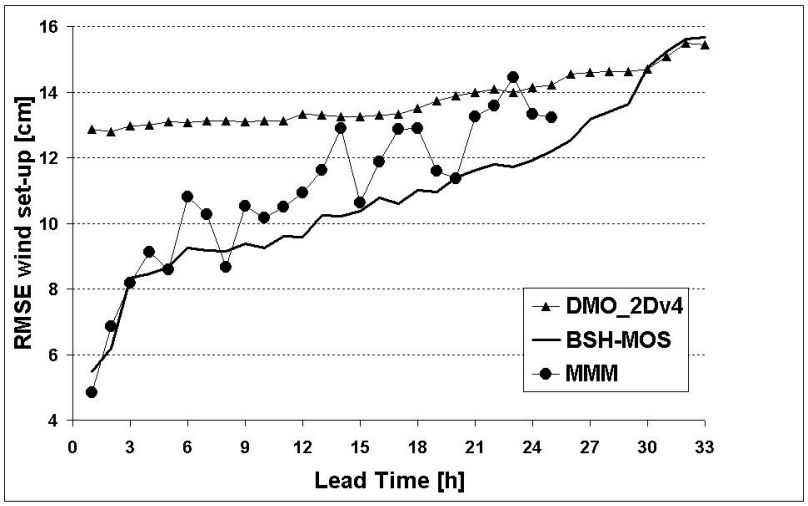

Fig. 4: RMSE of wind surge forecasts 15.07.2009–28.01.2010 {DMO_2Dv4: 23770 cases; BSH-MOS (Kombi): 20911, MMM: 2937}. RV of MMM: 28,5%.

Finally, the question remains as to the quality of BSH-MOS forecasts (here: Kombi) in comparison with independently made man-machine mix predictions (Fig. 4). To begin with, it should be noted that a period of 6½ months is rather short and, accordingly, 4 daily MMM reference values may cause major differences from one lead time to the next. As 2 of the 6½ verification months are relatively calm summer months, the RMSE level in Fig. 4 is a few centimetres lower than that in Fig. 2.

Apart from that, the behaviour of MMM is similar to that in Fig. 2, with the exception of the jumps at 6 and 14 h. Beyond 17 hours prediction time, it is hardly possible to improve DMO (2Dv4) by human intervention. However, it should be noted that the performance of BSH-MOS is better than that of MMM without major outliers, and it is only beyond 30 h prediction time that it cannot improve DMO further. The reason is that, due to technical problems with certain issue times, DMO cannot be used by regression for the longest lead times. This will be corrected in connection with the next software update.

It may be concluded from these findings that the automation potential of water level forecasts for the German coast is very good. Especially the hourly updates to the forecasts based on latest gauge data and four daily prediction runs of the modelling chain covering all pilotage waters and harbours in the German Bight would be beyond the capacity of a man-machine mix. Here, future use of BSH-MOS might lead to a quality boost.

6 Summary

In the BSH-MOS project, the BSH's physical and statistical expertise in water level forecasting for the German North Sea coast has been combined with the MSWR-MOS standard technology, which is quite mature by now. The approach of defining the initialisation error of DMO as a predictor has been particularly successful, because a measurement-based initial distribution covering the entire North Sea area cannot be constructed for the 2D North Sea surge model, which differs in this respect from the models used in weather forecasting. Therefore, the predicted distribution from the previous forecast for a corresponding period, i.e. a 6-hour prediction in each case, has to be used as initial distribution. Also the proposal to base the classification not on seasons, as is usually done, but on HW and LW or positive and negative surges led to a major additional improvement as far as developmental results are concerned. This would not have been possible by adhering rigidly to the MSWR-MOS standard technique, in which a limited number of surge predictors would have been defined and optimised. It will have to be investigated in what way these results open up opportunities for automating water level forecasting for the German North Sea coast.

Already now, the MOS equations found and the very good DMO allow the conclusion that complete automation may be possible at least in stable or slowly changing weather situations. All other weather situations – especially storm surge situations – will require human expertise in a man-machine mix also in the future (MÜLLER-NAVARRA, 2008).

Acknowledgment

The authors wish to thank Ms. Ingrid Lange (BSH) for her translation into English, and Mr. S. Palkowski (BSH) for providing to us the base data for operational use.

References

ANONYMUS, 1878: Gezeiten-Tafeln für die Deutsche Nordsee-Küste für das Jahr 1879. Kaiserliche Admiralität, Hydrographisches Bureau, Berlin: Mittler. 48 p.

CORKAN, R. H., 1950: The levels in the North Sea associated with the storm disturbance of 8 January 1949. Phil. Trans. Roy. Soc. London, Ser. A, Math. and Phys. Sci. 242, No 853. 493–525

DICK, S., KLEINE, E., MÜLLER-NAVARRA, S. H., KLEIN, H. AND KOMO, H., 2001: The Operational Circulation Model of BSH (BSHcmod) – Model description and validation. Berichte des Bundesamtes für Seeschifffahrt und Hydrographie 29, 48 S.

GERRITSEN, H., H. DE VRIES, AND M. PHILIPPART, 1995: The Dutch Continental Shelf Model. In: Quantitative Skill Assessment for Coastal Ocean Models, Coastal Estuarine Studies 47, edited by D. R. Lynch and C. N. K. Mooers, 425–467, AGU, Washington, D. C.

GLAHN, H. R. AND LOWRY, D. A., 1972: The use of model output statistics (MOS) in objective weather forecasting, J. Appl. Meteor. 11,1203–1211

HOFFMANN, J., 2008: Entwicklung und Anwendung von statistischen Vorhersage-Interpretationsverfahren für Gewitternowcasting und Unwetterwarnungen unter Einbeziehung von Fernerkundungsdaten. Berlin, Freie Univ., Diss., 207 S.

KALNAY, E., KANAMITSU, M., BAKER, W. E., 1990: Global numerical weather prediction at the National Meteorological Center. Bull. Amer. Meteor. Soc. 71. 1410–1428

KNÜPFFER, K., 1996: Methodical and Predictability Aspects of MOS Systems. Preprints from the 13th Conference on Probability and Statistics in the Atmospheric Sciences, Feb. 21–23, San Francisco, CA; American Meteorological Society pp. 19–23.

KNÜPFFER, K., 1997: Automation of Aviation Forecasts - The Projects AUTO-TAF and AUTO-GAFOR, Seventh Conference on Aviation, Range, and Aerospace Meteorology, 77th AMS Annual Meeting, Feb. 2–7, Long Beach, CA

KNÜPFFER, K., 1999: EMOS - a Milestone Towards Completely Automated Local Weather Forecasting. Proceedings of the 4th European Conference on Applications of Meteorology (ECAM 99), 13-17 September 1999, Norrkoeping, Sweden, CD-ROM.

KOLTERMANN, K.-P., W. LANGE, 1975: On the relation between residual currents and the wind field in the German Bight. Ocean Dynamics 28, 193–206

MAJEWSKI, D., D. LIERMANN, P. PROHL, B. RITTER, B. BUCHHOLD, T. HANISCH, G. PAUL, W. WERGEN, J. BAUMGARDNER, 2002: The Operational Global Icosahedral–Hexagonal Gridpoint Model GME: Description and High-Resolution Tests. Mon. Wea. Rev. 130, 319–338

MÜLLER-NAVARRA, S. H., 2008: Zur Vorhersagbarkeit schwerer Sturmfluten an deutschen Küsten. DMG-Mitteilungen 2/2008, 9–10

MÜLLER-NAVARRA, S. H., 2009a: Sturmfluten in der Elbe und deren Vorhersage im Wandel der Zeiten. Schriften der Deutschen Wasserhistorischen Gesellschaft (DWhG) e.V. Bd. 13, 77–95

MÜLLER-NAVARRA, S. H., 2009b: Automatic determination of tidal highs and lows in German Bight tidal curves (in German). Hydrologie und Wasserbewirtschaftung 53, 380–388

MÜLLER-NAVARRA, S. H., H. GIESE, 1999: Improvements of an Empirical Model to Forecast Wind Surge in the German Bight. Ocean Dynamics 51, 385–405

MÜLLER-NAVARRA, S. H., W. LANGE, S. DICK, K. C. SOETJE, 2003: Über die Verfahren der Wasserstands- und Sturmflutvorhersage: Hydrodynamisch-numerische Modelle der Nord- und Ostsee und empirisch-statistisches Verfahren für die Deutsche Bucht. promet 29, 117–124

ORTT, F. L., 1897: The effect of wind and atmospheric pressure on the tides. Nature 56, 80–84

RUDOLPH, E., 2005: Einfluss sehr hoher Abflüsse auf die Wasserstände in der Tideelbe. promet 31, 186–190.

SCHERHAG, R., 1948: Neue Methoden der Wetteranalyse und Wetterprognose. Springer Verlag, Berlin. 424 S.

SOETJE, K. C., C. BROCKMANN, 1983: An operational numerical model of the North Sea and the German Bight. In: J. SÜNDERMANN/W. LENZ (Ed.): North Sea Dynamics. 95–107

STEPPELER, J., G. DOMS, U. SCHÄTTLER, H. W. BITZER, A. GASSMANN, U. DAMRATH, G. GREGORIC, 2003: Meso-Gamma Scale Forecasts Using the Non-hydrostatic Model LM. Meteorology and Atmospheric Physics 82, 75–90

Berichte des Bundesamtes für Seeschifffahrt und Hydrographie

Verzeichnis der veröffentlichten Arbeiten

1	(1994)	Sy, A., Ulrich, J.	North Atlantic Ship-of-Opportunity XBT Programme 1990 – Data Report, 134 pp.
2	(1994)	Hagen, E., Mittelstaedt, E., Feistel, R., Klein, H.	Hydrographische Untersuchungen im Ostrandstromsystem vor Portugal und Marokko 1991–1992, 49 pp.
3	(1994)	Oliczewski, J., Schmidt, D.	Entwicklung einer Bestrahlungsapparatur zum photochemischen Aufschluß von Meerwasserproben zur Bestimmung von Schwermetallen, 70 pp.
4	(1994)	BSH [Hrsg.]	Das UN-Seerechtsübereinkommen tritt in Kraft: Inhalte und Konsequenzen für die Bundesrepublik Deutschland, 71 pp.
5	(1995)	BSH [Hrsg.]	Nationale Folgerungen aus dem Inkrafttreten des UN-Seerechts-übereinkommens, 103 pp.
6	(1995)	Haffer, E., Schmidt, D.	Entwicklung eines Probenvorbereitungsverfahrens zur Bestimmung von Arsen im Meerwasser mit der Totalreflexions-Röntgenfluoreszenzanalyse, 109 pp.
7	(1995)	BSH [Hrsg.]	Global Ocean Observing System – Statusbericht, 100 pp.
8	(1996)	Mittelstaedt, E., Meincke, J., Klein, H.	WOCE-Current measurements: The ACM8 array – Data Report, 150 pp.
9	(1996)	BSH [Hrsg.]	GOOS Workshop – Anforderungen an ein wissenschaftliches Konzept für den deutschen Beitrag, 60 pp.
10	(1997)	Sterzenbach, D.	Entwicklung eines Analyseverfahrens zur Bestimmung von chlorierten Kohlenwasserstoffen in marinen Sedimenten und Schwebstoffen unter besonderer Berücksichtigung der überkritischen Fluidextraktion, 233 pp.
11	(1997)	Jonas, M., Richter, R.	Stand und Entwicklungstendenzen nautischer Systeme, Anlagen und Geräte an Bord von Seeschiffen, 37 pp.
12	(1997)	Wedekind, C., Gabriel, H., Goroncy, I., Främke, G., Kautsky, H.	„Meteor"-Reise Nr. 71/1985, Norwegen–Grönlandsee – Datenbericht, 44 pp.
13	(1998)	BSH [Hrsg.]	HELCOM Scientific Workshop – The Effects of the 1997 Flood of the Odra and Vistula Rivers, 46 pp.
14	(1998)	Berger, R., Klein, H., Mittelstaedt, E., Ricklefs, K., Ross, J.	Der Wasseraustausch im Tidebecken Hörnum-Tief – Datenreport, 260 pp.
15	(1998)	Röske, F.	Wasserstandsvorhersage mittels neuronaler Netze. 212 pp.
16	(1998)	Ross, J., Mittelstaedt, E., Klein, H., Berger, R., Ricklefs, K.	Der Wasseraustausch im Tidebecken Hörnum-Tief – Abschlußbericht, 98 pp.
17	(1998)	Klein, H.	OPUS-Current Measurements: Mecklenburg Bight and Fehmarnbelt – Data Report, 150 pp.
18	(1999)	BSH [Hrsg.]	Deutscher Programmbeitrag zum Globalen Ozeanbeobachtungssystem (GOOS), 67 pp.
19	(1999)	BSH [Hrsg.]	German Programme Contribution to the Global Ocean Observing System (GOOS), 71 pp.
20	(1999)	Sztobryn, M., Stanislawczyk, I., Schmelzer, N.	Ice Conditions in the Szczecin and Pomeranian Bay During the Normal Period from 1961–1990, 36 pp.
21	(1999)	Nies, H., Karcher, M., Bahe, C., Backhaus, J., Harms, I.	Transportmechanismen radioaktiver Substanzen im Arktischen Ozean – Nummerische und experimentelle Studien am Beispiel der Barents- und Karasee, 134 pp.
22	(2000)	Lorbacher, K.	Niederfrequente Variabilität meridionaler Transporte in der Divergenzzone des nordatlantischen Subtropen- und Subpolarwirbels – Der WOCE-Schnitt A2, 156 pp.

23	(2000)	Klein, H.	The Subsurface Eastern Boundary Current of the North Atlantic between 32° N and 53° N – Data Report, 240 pp.
24	(2000)	Klein, H.	Strömungen und Seegangsverhältnisse westlich der Insel Hiddensee – Datenreport, 59 pp.
25	(2001)	Goedecke, E.	Der hydrographische Aufbau in der Deutschen Bucht vornehmlich dargestellt auf Grund der vorliegenden Unterlagen über Temperatur, Salzgehalt und Dichte, 202 pp.
26	(2001)	Klein, H., Mittelstaedt, E.	Strömungen und Seegangsverhältnisse vor Graal-Müritz und in der Tromper Wiek – Datenreport, 162 pp.
27	(2001)	Klein, H., Mittelstaedt, E.	Gezeitenströme und Tidekurven im Nahfeld von Helgoland, 24 pp. und Anhang.
28	(2001)	Behnke, J., Berking, B., Herberg, J., Jonas, M., Mathes, S.	Functional Scope and Model of Integrated Navigation Systems – A Toolbox for Identification and Testing, 181 pp.
29	(2001)	Dick, S., Kleine, E., Müller-Navarra, S., Klein, H., Komo, H.	The Operational Circulation Model of BSH (BSHcmod) – Model description and validation, 49 pp.
30	(2002)	Sy, A., Ulrich, J., Weichert, H.-J.	Upper Ocean Climate Ship-of-Opportunity Programme of BSH – A Status Report, 45 pp.
31	(2003)	Dahlmann, G.	Characteristic Features of Different Oil Types in Oil Spill Identification, 48 pp.
32	(2003)	Nies, H., Gaul, H., Oestereich, F., Albrecht, H., Schmolke, S., Theobald, N., Becker, G., Schulz, A., Frohse, A., Dick, S., Müller-Navarra, S., Herklotz, K.	Die Auswirkungen des Elbehochwassers vom August 2002 auf die Deutsche Bucht, 81 pp.
33	(2003)	Loewe, P., Becker, G., Brockmann, U., Frohse, A., Herklotz, K., Klein, H., Schulz, A.	Nordsee und Deutsche Bucht 2002 – Ozeanographischer Zustandsbericht
34	(2004)	Schulz, G.	Geomagnetic Results Wingst 1996, 1997, 1998 and 1999 including the complete Wingst data set since 1939 on CD-ROM
35	(2004)	Gouretski, V. V., Koltermann, K. P.	WOCE Global Hydrographic Climatology
36	(2004)	Gayer, G., Dick, S., Pleskachevsky, A., Rosenthal, W.	Modellierung von Schwebstofftransporten in Nord- und Ostsee
37	(2004)	Schmelzer, N., Strübing, K., Stanisławczyk, I., Sztobryn, M.	Die Eiswinter 1999/2000 bis 2003/2004 an der deutschen Nord- und Ostseeküste/Ice Conditions in the Szczecin Lagoon and Pomeranian Bay During the Winters 1999–2002
38	(2005)	Loewe, P., Schmolke, S., Becker, G., Brockmann, U., Dick, S., Engelke, C., Frohse, A., Horn, W., Klein, H., Müller-Navarra, S., Nies, H., Schmelzer, N., Schrader, D., Schulz, A., Theobald, N., Weigelt, S.	Nordseezustand 2003
39	(2005)	Sztobryn, M., Stigge, H.-J., Wielbińska, D., Stanisławczyk, I., Kańska, A., Krzysztofik, K., Kowalska, B., Letkiewicz, B., Mykita, M., Weidig, B.	Sturmfluten in der südlichen Ostsee (westlicher und mittlerer Teil)/ Storm Surges in the Southern Baltic Sea (Western and Central Parts)
40	(2006)	Loewe, P., Schmolke, S., Becker, G., Brockmann, U., Dick, S., Frohse, A., Herrmann, J., Klein, B., Klein, H., Nies, H., Schrader, D., Schulz, A., Theobald, N., Weigelt, S.	Nordseezustand 2004
41	(2007)	Bork, I., Dick, S., Kleine, E., Müller-Navarra, S.	Tsunami – a study regarding the North Sea coast
42	(2007)	Schrum, C., Schmelzer, N. (Eds.)	Fifth Workshop on Baltic Sea Ice Climate Hamburg, Germany, 31 August–2 September 2005

43	(2008)	Müller, L.	Sauerstoffdynamik der Nordsee – Untersuchungen mit einem dreidimensionalen Ökosystemmodell
44	(2009)	Loewe, P. (Ed.)	System Nordsee – Zustand 2005 im Kontext langzeitlicher Entwicklungen
45	(2009)	Sztobryn, M., Weidig, B., Stanisławczyk, I., Holfort, J., Kowalska, B., Mykita, M., Kańska, A., Krzysztofik, K., Perlet, I.	Niedrigwasser in der südlichen Ostsee (westlicher und mittlerer Teil)/ Negative Surges in the Southern Baltic Sea (Western and Central Parts)
46	(2009)	Schmelzer, N., Holfort, J.	Eiswinter 2004/05 bis 2008/09 an den deutschen Nord- und Ostseeküsten Ice Winters 2004/05 to 2008/09 on the German North and Baltic Sea Coasts
47	(2010)	Müller-Navarra, S., Knüpffer, K.	Improvement of water level forecasts for tidal harbours by means of model output statistics (MOS) – Part I (Skew surge forecast)